PB89-236376

Calcium Oxide Sintering in Atmospheres Containing Water and Carbon Dioxide

(U.S.) Environmental Protection Agency, Research Triangle Park, NC

1989

U.S. Department of Commerce
National Technical Information Service
NTIS

AEERL-P-398

TECHNICAL REPORT DATA
(Please read Instructions on the reverse before complet

1. REPORT NO. EPA/600/J-89/009	2.	3. PB89-236376
4. TITLE AND SUBTITLE: Calcium Oxide Sintering in Atmospheres Containing Water and Carbon Dioxide		5. REPORT DATE 6. PERFORMING ORGANIZATION CODE
7. AUTHOR(S): Robert H. Borgwardt		8. PERFORMING ORGANIZATION REPORT NO.
9. PERFORMING ORGANIZATION NAME AND ADDRESS: See Block 12		10. PROGRAM ELEMENT NO. 11. CONTRACT/GRANT NO. NA
12. SPONSORING AGENCY NAME AND ADDRESS: **EPA, Office of Research and Development** **Air and Energy Engineering Research Laboratory** **Research Triangle Park, NC 27711**		13. TYPE OF REPORT AND PERIOD COVERED: Journal article; 10/86 - 9/87 14. SPONSORING AGENCY CODE: **EPA/600/13**

15. SUPPLEMENTARY NOTES: AEERL project officer is Robert H. Borgwardt, Mail Drop 4, 919/541-2336. In: Ind. Eng. Chem. Res., Vol. 28, No. 4, pp. 493-500, April 1989.

16. ABSTRACT: The paper gives results of measurements of the effects of water vapor and CO2 on the sintering rate of nascent CaO, as a function of partial pressure and temperature using CaO prepared by rapid decomposition of CaCO3 and Ca(OH)2. Each gas strongly catalyzed the sintering process and their combined effects were additive. A model formulated by R. M. German and Z. A. Munir in 1976, which describes surface area reduction by a single mechanism, is empirically modified to account for catalytic effects of the gas phase. Although multiple sintering mechanisms are apparently operative in the presence of CO2 and/or H2O, the empirical model correlates isothermal surface area reduction as a function of time over the temperature range of 380 to 1150 C and partial pressures of 39 Pa to 15 kPa. Porosity reduction was also accelerated by the presence of H2O or CO2 in the sintering atmosphere. In an atmosphere of simulated flue gas, porosity reduction followed the Coble logarithmic law during sintering at 800, 900, and 1000 C with induction periods of 6, 4.5, and 2.7 sec, respectively, for onset of particle shrinkage. Coupling the sintering model with a sulfation model that accounts for the effects of surface area allows the prediction of SO2 capture efficiencies in boiler furnaces by Ca(OH)2 injection.

17. KEY WORDS AND DOCUMENT ANALYSIS

a. DESCRIPTORS		b. IDENTIFIERS/OPEN ENDED TERMS	c. COSATI Field/Group	
Pollution	Sulfur Dioxide	Pollution Control	13B	
Calcium Oxides	Calcium Hydroxides	Stationary Sources	07B	
Sintering	Flue Gases		13H	21B
Sulfation	Furnaces		07C	13A
Water	Porosity			14G
Carbon Dioxide	Mathematical Models			12A

18. DISTRIBUTION STATEMENT: **Release to Public**	19. SECURITY CLASS *(This Report)* **Unclassified**	21. NO. OF PAGES 10
	20. SECURITY CLASS *(This page)* **Unclassified**	22. PRICE

EPA Form 2220-1 (9-73)

REPRODUCED BY
U.S. DEPARTMENT OF COMMERCE
NATIONAL TECHNICAL INFORMATION SERVICE
SPRINGFIELD, VA. 22161

EPA/600/J-89/009
Published in I&EC Research, April 1989, 493–500, by the American Chemical Society

Calcium Oxide Sintering in Atmospheres Containing Water and Carbon Dioxide

NTIS is authorized to reproduce and sell this report. Permission for further reproduction must be obtained from the copyright owner.

Robert H. Borgwardt

Air and Energy Engineering Research Laboratory, U.S. Environmental Protection Agency, Research Triangle Park, North Carolina 27711

The effects of water vapor and CO_2 on the sintering rate of nascent calcium oxide were measured as a function of partial pressure and temperature using CaO prepared by rapid decomposition of $CaCO_3$ and $Ca(OH)_2$. Each gas strongly catalyzed the sintering process, and their combined effects were additive. The model formulated by German and Munir, which describes surface area reduction by a single mechanism, is empirically modified to account for catalytic effects of the gas phase. Although multiple sintering mechanisms are apparently operative in the presence of CO_2 and/or H_2O, the empirical model correlates isothermal surface area reduction as a function of time over the temperature range 380–1150 °C and partial pressures of 39 Pa to 15 kPa. Porosity reduction was also accelerated by the presence of H_2O or CO_2 in the sintering atmosphere. In an atmosphere of simulated flue gas, porosity reduction followed the Coble logarithmic law during sintering at 800, 900, and 1000 °C with induction periods of 6, 4.5, and 2.7 s, respectively, for the onset of particle shrinkage. A coupling of the sintering model with a sulfation model that accounts for the effects of surface area allows the prediction of SO_2 capture efficiencies in boiler furnaces by $Ca(OH)_2$ injection.

In an effort to minimize the cost of flue gas desulfurization and increase the range of options available to industry for pollution control, several processes based on the injection of limestone-derived sorbents are being evaluated. This approach appears to be the most effective one for application to existing plants because of its relative ease of retrofit. Several alternative sorbents and modes of injection are under trial; the one of interest here is injection into the furnace at temperatures up to 1230 °C where the particles calcine and the CaO reacts with SO_2 during the short residence time (ca. 2 s) before the temperature cools and reaction ceases. Successful application of this process to boilers of varied design, each operating at different conditions, requires a predictive model that accounts for the rate processes involved. Prior work has shown that the calcination of small $CaCO_3$ particles produces a nascent CaO of high initial surface area (Borgwardt, 1985) and that the SO_2 reaction rate of this CaO is strongly related to its specific surface area (Borgwardt and Bruce, 1986) when the particles are sufficiently small to minimize pore diffusion resistance.

At the high temperatures required for fast SO_2 reaction, CaO sintering kinetics must be considered. A preliminary study of CaO sintering (Borgwardt, 1989) showed that the initial surface areas, S_0, of nascent CaO produced by the decomposition of $CaCO_3$ and $Ca(OH)_2$ are 104 and 76.7 m^2/g, respectively. The measured rates of surface area reduction in a nitrogen atmosphere were correlated by the model of German and Munir (1976):

$$\left(\frac{S_0 - S}{S_0}\right)^{\gamma} = K_i t \qquad (1)$$

where γ is a mechanism-dependent parameter and K_i is a sintering constant that increases exponentially with temperature. The data analysis yielded a value of $\gamma = 2.7$, corresponding to lattice diffusion, as the sintering mechanism in an inert atmosphere. Porosity declined logarithmically with time during the intermediate stage of sintering according to the model of Coble (1961):

$$\epsilon_0 - \epsilon = k_p \ln (t/t_i) \qquad (2)$$

This paper addresses the effects of H_2O and CO_2, which are major constituents of flue gas, on CaO sintering. The effect of water vapor on surface area reduction in MgO is well documented by Anderson and Morgan (1964) and Anderson et al. (1965). They propose that the effect arises from surface diffusion induced by adsorbed H_2O and discuss several possible mechanisms. The latter study further showed that surface reduction in CaO is more sensitive to water vapor than MgO and that the reduction is due to crystallite growth, not merely agglomeration and closure of pores. The effect of H_2O on the loss of surface area and porosity of silica is also known (Schlaffer et al., 1965). The reduction of porosity as well as surface area in silica suggests that more than one mechanism of sintering can be affected.

CO_2 also accelerates CaO sintering. O'Neill et al. (1976) found that calcination in atmospheres containing CO_2 increases the reactivity of large $CaCO_3$ particles with SO_2, an effect which Ulerich et al. (1978) related to enlargement of the CaO pore size. This effect implies a role of CO_2 in sintering, and since it occurs above the dissociation temperature of $CaCO_3$, the mechanism is catalytic. Beruto et al. (1984) demonstrated the catalytic effect by measurements of surface area and porosity reduction in CaO exposed at 686 °C to CO_2 well below the equilibrium pressure required for $CaCO_3$ formation. The catalysis was attributed to enhancement of surface diffusion by reversible chemisorption of CO_2, analogous to the mechanism for H_2O-catalyzed sintering postulated by Anderson and Morgan (1964). An experimental method suitable for measurement of CaO surface area reduction, as a function of temperature and gas composition, has been reported (Borgwardt et al., 1986). That method is applied here to determine sintering kinetics in the presence of both CO_2 and H_2O.

Because of the strong effect of pore diffusion resistance at high reaction temperature, especially with high-surface CaO, minimum particle size is required for efficient sorbent utilization with furnace injection. Hydrated lime, which has a smaller mean particle size than finely ground limestone (ca. 2 versus 10 μm), is therefore the sorbent of choice and is emphasized in this work, although comparisons with limestone-derived CaO are included to generalize results.

A recent study by Mai (1987) is the most detailed analysis of H_2O and CO_2 effects on the sintering of hydroxide-derived CaO. That work was done in a dis-

persed-particle flow reactor at 1010 and 1150 °C in which resident times were less than 3 s. Individual and combined effects of H_2O and CO_2 on CaO surface area reduction were demonstrated. A model based on Nicholson's (1965) sintering formula was used for correlation, a model which requires prior knowledge of terminal surface areas as a function of temperature—with or without the presence of H_2O or CO_2—for application to nonisothermal systems. A different model that is based on the initial properties of the sorbent and predicts S as a function of time would be more adaptable to the problem at hand and is the objective of the work reported here. An additional objective is to relate the surface area reductions observed in time scales of a few seconds at high temperature to the better understood sintering processes occurring much more slowly in uncatalyzed atmospheres.

Experimental Section

To slow sintering to manageable rates and extend the time periods over which measurements can be made, differential reactors were used. Two such reactors, previously described (Borgwardt, 1985; Borgwardt et al., 1986), were mounted adjacently. One reactor was used exclusively for calcination at 700 °C, the second reactor for sintering. These methods permit the use of small (25-mg) samples and small particles (to 1 μm) of sorbent, dispersed in a quartz wool substrate. Fourteen such samples were calcined, sintered, and composited for each surface area analysis. Multipoint BET analyses of surface area were made with a Micromeritics Accusorb by N_2 adsorption. To determine the precise CaO content, each BET flask was extracted with dilute HCl after surface area measurement and the calcium titrated with EDTA.

Porosity measurement required larger samples, which were prepared by calcining 250 mg of $Ca(OH)_2$ or $CaCO_3$, sintering each calcine, and compositing six calcines for analysis in a Micromeritics automated Digisorb. This instrument determines pore volume by N_2 condensation at relative pressures approaching saturation at liquid N_2 temperature. At a relative pressure of 0.99, where these measurements were made, pores up to 0.19-μm diameter are included. Most of the intraparticle pore volume is thus accounted for while excluding interparticle voids.

Gas flow through the sintering reactor was continued at a constant rate of 6 L/min throughout the sinter period. Sintering in H_2O atmospheres was conducted by passing N_2 gas (from a liquid N_2 tank) through flasks of water suspended in a constant-temperature bath and a heat-traced feed line to the sintering reactor. Partial pressures were verified by measurement of weight gain of Drierite. Low partial pressures were obtained by N_2 dilution and by double dilution as described by Nelson (1971). CO_2 was added after humidification when both components were tested.

The limestone used here was the same Fredonia used in the prior sintering tests made in a N_2 atmosphere. Except where otherwise noted, the particle size of the limestone was 10 μm. The principal hydroxide was Presque Isle commercial $Ca(OH)_2$ produced in Michigan. Fisher analytical grade $Ca(OH)_2$ was included as a reference material. The lower decomposition temperature of $Ca(OH)_2$ relative to $CaCO_3$ requires a compromise on the choice of calcination conditions in order to compare their CaO products. Decomposition of the hydroxide in N_2 proceeds at an appreciable rate at 370 °C, using the method employed here, yielding CaO with a surface area of 128 m^2/g—in agreement with the value reported by Anderson et al. (1965) for calcination under vacuum. When these calcines were transferred to the second reactor at 700 °C, the surface area immediately collapsed to 77 m^2/g in less than 15 s, or within the minimum time required for heat-up. Once this lower surface area was reached, further reduction proceeded much more slowly (ΔS = 14 m^2/g in 18 min at 700 °C). The true sintering rate was therefore not related to the initial collapse.

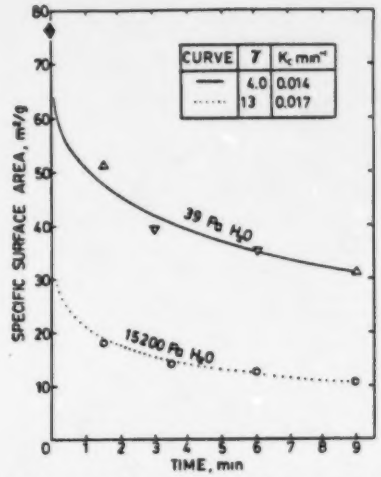

Figure 1. Surface area reduction at 800 °C in atmospheres of water vapor in N_2. CaO prepared from commercial hydroxide (○, △) and analytical grade hydroxide (▽). Curves are eq 1 with indicated values providing best fit.

It is possible that the CaO formed at the lower temperature exists as platelets in the manner that MgO platelets are formed by $Mg(OH)_2$ decomposition at 300 °C (Anderson and Morgan, 1964). At 700 °C such platelets may contract to spherical grains prior to the onset of sintering. This interpretation is plausible only if the atoms comprising the platelets have not yet arranged into a CaO lattice. Because 700 °C was used for $CaCO_3$ calcination in the prior work and is closer to the injection temperature of practical interest, the procedure used for hydroxide calcination was to insert the samples in the reactor at 700 °C with N_2 flowing (no heat-up period). Calcination was continued in flowing N_2 (20 L/min) for 5 min; then the sample was transferred to the sintering reactor.

Results

Since, in the presence of H_2O and CO_2, sintering is a catalyzed process involving multiple transport mechanisms, eq 1 does not strictly apply. It is to be shown that the German–Munir model can nevertheless correlate data for isothermal sintering catalyzed by H_2O and CO_2. For this purpose, the rate constant K_i of eq 1, for sintering in an inert atmosphere, is replaced by the parameter K_c-(T,P_{H_2O},P_{CO_2}). It is understood that the value of γ can also change with gas composition and temperature as more than one mechanism becomes operative. The object of the following study is to evaluate the two sintering parameters, K_c and γ, in a manner that will permit extrapolation to higher temperatures and predict S at sintering times of a few seconds. Since the approach is empirical, the values of K_c and γ no longer have significance regarding the sinter mechanism.

Acceleration of Surface Area Reduction by H_2O. Figures 1 and 2 are the results of isothermal (800 °C) sintering tests made at various H_2O partial pressures using CaO prepared from $Ca(OH)_2$ and limestone, respectively. The sintering rate is strongly affected by the presence of a very small concentration of water vapor, in agreement with the result reported by Anderson and Morgan (1964)

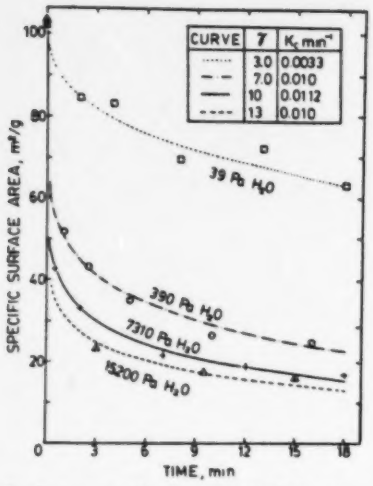

Figure 2. Surface area reduction at 800 °C in atmospheres containing water vapor in N_2. CaO prepared from 10-μm limestone.

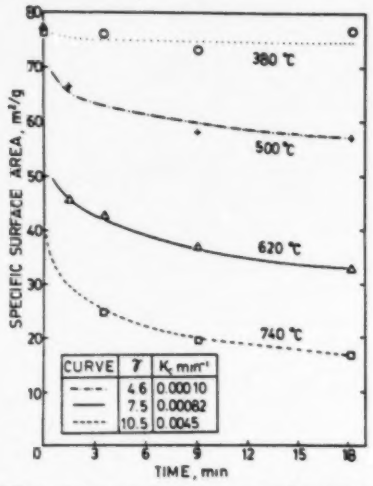

Figure 3. Effect of sinter temperature on surface area reduction in an atmosphere of 7.3 kPa of H_2O. CaO prepared from commercial hydroxide.

for MgO sintering. The curves are eq 1 with values of γ and K_c determined by best fit. They show that increasingly higher γ values are required to fit the data as P_{H_2O} is raised. This result is attributed to other diffusion mechanisms occurring in addition to the lattice diffusion which takes place in the absence of H_2O. The highest γ values for single-mechanism transport are 3.3 and 3.5, corresponding to grain boundary and surface diffusion. The data do not show a clear dependence of K_c on P_{H_2O}.

Temperature Effect with Constant P_{H_2O}. Surface area reduction rates of CaO prepared from $Ca(OH)_2$ and limestone are compared in Figures 3 and 4 for tests made in a sintering atmosphere containing 7.3 kPa of H_2O in N_2, which is within the normal range of H_2O in combustion gases from coal-fired furnaces. The presence of H_2O markedly reduced the temperature at which surface reduction begins: from 700 °C in a N_2 atmosphere to 440 °C in 7.3 kPa of H_2O (7.2 vol %).

The K_c values determined by fitting eq 1 to these data are plotted in Figure 5 according to the Arrhenius equation. Both types of CaO can be represented by a single straight line:

$$\ln K_c = (-11660/T) + 6.25 \qquad (3)$$

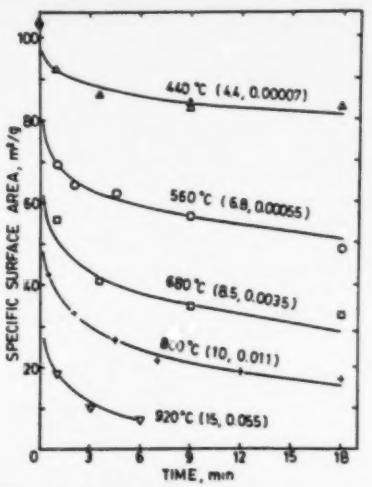

Figure 4. Effect of sinter temperature on surface area reduction in an atmosphere of 7.3 kPa of H_2O. CaO prepared from 10-μm limestone. Values in parentheses are γ and K_c, respectively, used in eq 1 to obtain the curves shown.

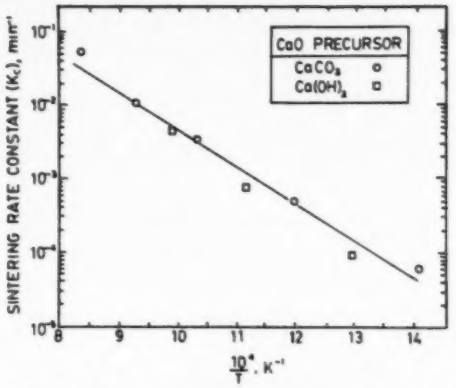

Figure 5. Arrhenius plot of pseudosintering rate constants from Figures 3 and 4. Effect of temperature evaluated at constant P_{H_2O} = 7.3 kPa.

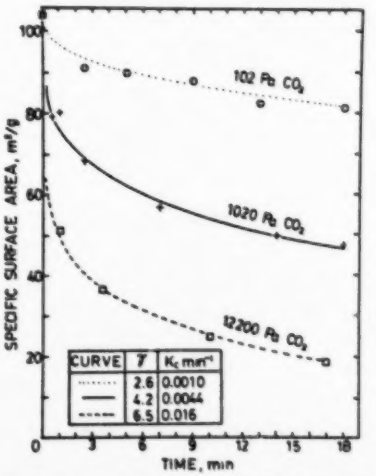

Figure 6. Surface area reduction at 800 °C in atmospheres containing CO_2 in nitrogen. CaO prepared from 10-μm limestone.

Acceleration of Surface Reduction by CO_2. Carbon dioxide also catalyzes CaO surface reduction as shown by Figure 6. At normal flue gas partial pressure (12.2 kPa of CO_2), its effect is less than that of H_2O. Figure 7 shows

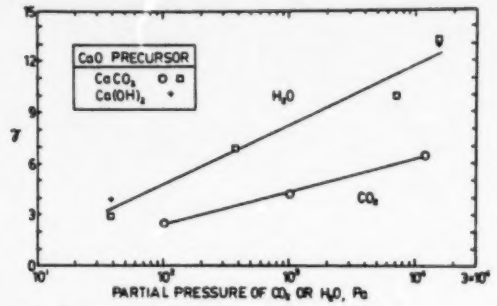

Figure 7. Effect of partial pressure on γ at 800 °C.

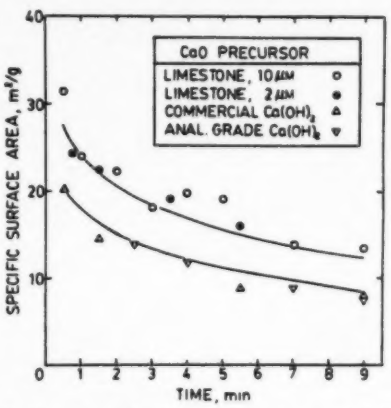

Figure 8. Surface area reduction in atmosphere containing 7.3 kPa of H_2O + 12.2 kPa of CO_2 at 800 °C.

the relationship between partial pressure and γ as determined from the data of Figures 1, 2, and 6 for both CO_2 and H_2O. K_c is also dependent on P_{CO_2}. A log–log plot of K_c versus P_{CO_2} (from Figure 6) yields the following relationship at 800 °C:

$$K_c = 0.0040 P_{CO_2}^{0.558} \quad (4)$$

Combined Effect of H_2O and CO_2 on Surface Reduction. Figure 8 compares the two types of CaO in a simulated flue gas of 7.3 kPa of H_2O, 12.2 kPa of CO_2, and balance N_2. It is apparent from Figures 1, 7, and 8 that the effects of CO_2 and H_2O are additive; i.e., CaO sinters faster in flue gas than in either H_2O or CO_2 independently. Supplementary experiments were made with limestone of 2-μm particle size to verify that the differences between the apparent sintering rates of limestone CaO and hydroxide CaO indicated by Figure 8 were not due to a particle size effect. Those results, indicated by closed symbols in Figure 8, revealed no effect of particle size on sintering rate, as was the case in a N_2 atmosphere.

The solid curves in Figure 8 are drawn with a single value of $\gamma = 15.5$ and $K_c = 0.016$, which give the minimum overall deviation from the combined data of both sets. This procedure is consistent with the conclusion that K_c and γ are independent of CaO type, although a slightly better fit is obtained by treating the two sets of data independently. The difference between the sintering rates of hydroxide CaO and limestone CaO in flue gas, like the difference found in pure N_2 (Borgwardt, 1989), is attributable to the lower ϵ_0 and S_0 values of the hydroxide CaO.

Comparison with High-Temperature Data. It is apparent from Figures 3 and 4 that γ, as well as K_c, increases with temperature. The relationship is shown in Figure 9. Using Mai's (1987) high-temperature data to extend the range of correlation, it is found that the γ values

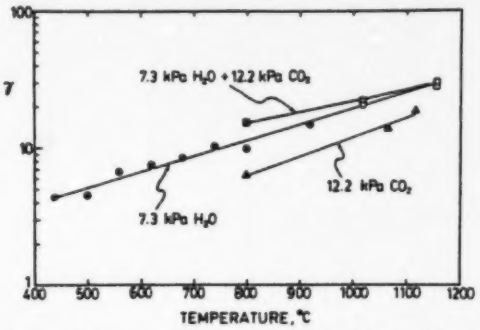

Figure 9. Effect of sintering temperature and atmosphere on γ.

Table I. Porosity of CaO Sintered 6 min at 800 °C

	CaO precursor[a]	
sintering atmosphere	2-μm limestone	commercial $Ca(OH)_2$
nitrogen	0.48	0.40
7.3 kPa of H_2O	0.41	0.36
12.2 kPa of CO_2	0.39	0.32
7.3 kPa of H_2O + 12.2 kPa of CO_2	0.35	0.22

[a] Calcined at 700 °C.

in 7–8 kPa of H_2O atmosphere follow the empirical relationship

$$\ln \gamma_{H_2O} = 0.00262T - 0.395 \quad (5)$$

Mai's data, plotted as open symbols in Figure 9, were obtained by extrapolation of the straight line of Figure 5 to obtain K_c values at the higher temperatures. These values were used in eq 1 with Mai's measurements of S at times of 1–3 s, to obtain γ for tests made in atmospheres containing 7.9 kPa of H_2O.

The data for CO_2 atmosphere = 12.2 kPa in Figure 9 were obtained from a different isothermal flow reactor, operated as part of this study, in which 10-μm limestone particles were calcined and sintered 0.3–0.6 s at 1068 and 1116 °C, respectively. The use of limestone rather than hydroxide for this experiment avoids potential interference of H_2O that is present during hydroxide decomposition. The top line in Figure 9 is obtained from the data of Figure 8 and Mai's data for flue gas atmospheres. The three lines are empirically related by

$$\gamma_{H_2O+CO_2} = 0.376(\gamma_{H_2O} + \gamma_{CO_2}) + 8.8 \quad (6)$$

Porosity Reduction. The porosities of CaO prepared from 2-μm limestone and Presque Isle hydroxide are compared in Table I as determined after 6 min of sintering in atmospheres of N_2, CO_2, H_2O, and $CO_2 + H_2O$. In each case, the sinter temperature was 800 °C, which is 40 °C above the equilibrium temperature for $CaCO_3$ decomposition in the presence of 12.2 kPa of CO_2. Although no stable reaction product can form at these conditions, the results show a clear effect of both CO_2 and H_2O on the reduction of CaO porosity. Like the surface area effect, a combination of H_2O and CO_2 in the sintering atmosphere has a greater effect than either gas individually.

In Figure 10, the porosity of hydroxide CaO is plotted as a function of time when sintered in a simulated flue gas atmosphere. As was the case for limestone CaO sintered in nitrogen (Borgwardt, 1989), the porosity reduction is well represented by the Coble law, eq 2, at each of the three sintering temperatures evaluated. Extrapolation of these lines to $\epsilon_0 = 0.49$ (the theoretical porosity before shrinkage) yields induction periods of 6, 4.5, and 2.7 s at 800, 900, and 1000 °C, respectively.

Table II. Evaluation of Sinter Model in Isothermal Systems

CaO precursor	sinter time, min	temp, °C	P_{H_2O}, kPa	P_{CO_2}, kPa	surface area, m^2/g predicted	surface area, m^2/g meas'd	error, %
$CaCO_3$	2.0	800	7.3	12.2	20.8	22.5	7.6
	7.0	800	7.3	12.2	13.8	14.0	1.4
$Ca(OH)_2$	0.5	800	7.3	12.2	20.6	21.8	5.5
	4.0	800	7.3	12.2	12.5	11.6	7.8
$Ca(OH)_2$[a]	0.040	1156	8.3	13.3	11.7	10.9	7.3
	0.039	1018	3.9	13.2	17.9	17.8	0.6
	0.040	1156	4.0	18.3	11.6	10.9	6.4
	0.040	1018	8.2	13.3	17.3	16.6	4.2
$CaCO_3$	0.0095	1068	0	12.2	35.8	41.3	13.3
	0.0055	1116	0	12.2	32.3	33.5	3.6
$Ca(OH)_2$[a]	0.017	1156	4.06	0	15.6	15.5	0.6
	0.040	1156	4.06	0	13.6	15.5	12.2
	0.017	1012	8.1	0	22.5	19.5	15.4
	0.040	1012	8.1	0	20.2	19.5	3.6
	0.040	1156	8.3	13.3	11.7	10.2	14.7
$CaCO_3$	9	440	7.3	0	87.0	84.4	3.0
	9	560	7.3	0	62.9	56.8	10.7
	9	680	7.3	0	38.5	34.8	10.6
	12	800	7.3	0	18.0	18.9	4.8
	9	800	0	0.102	90.4	88.2	2.5
	7	800	0	1.02	59.4	57.1	4.0
	10	800	0	12.2	26.2	25.4	3.1
$Ca(OH)_2$	9	380	7.3	0	70.5	73.4	4.0
	9	500	7.3	0	55.8	58.5	5.1
	9	620	7.3	0	37.0	36.8	5.0
	9	740	7.3	0	20.9	19.8	5.5

[a] Data of Mai (1987).

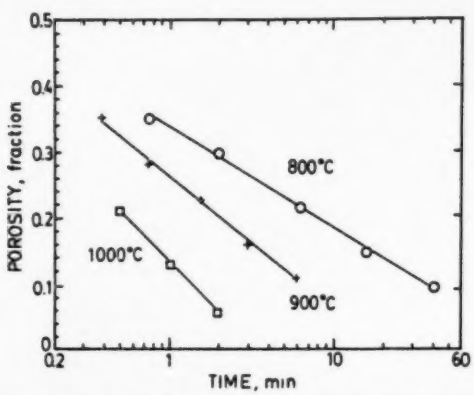

Figure 10. Porosity reduction in an atmosphere of 7.3 kPa of H_2O + 12.2 kPa of CO_2. CaO prepared from commercial hydroxide at 700 °C.

Discussion

The reactivity of CaO with SO_2 will be affected by reductions of either porosity or surface area by sintering. Prior studies (Beruto et al., 1984; Borgwardt, 1989) showed that the initial stage of CaO sintering is characterized by a rapid reduction of surface area with little change in porosity. The initial stage is followed by an intermediate stage in which both surface area and porosity decline. The time required for onset of the intermediate stage is defined by the induction period, t_i, which can be estimated by extrapolation of the porosity data to the initial (theoretical) value, ϵ_0, according to the Coble logarithmic law, eq 2. Extrapolation of the data of Figure 10 to shorter times indicates that the induction period is about 2.7 s at 1000 °C. The corresponding ΔS in that period is 78%. Under furnace injection conditions, the loss of surface area thus appears to be of predominant importance in establishing the physical properties of the solid that affect initial reaction rate.

The results of this study confirm the conclusions of Mai regarding the qualitative effects of CO_2 and H_2O on surface reduction: (1) it is accelerated by either of these constituents in the sintering atmosphere; (2) at a given partial pressure, H_2O has the greater effect, and (3) combinations of the two gases have a stronger effect than either individually. It is to be shown that their effects can be correlated over a broad range of temperatures and partial pressures, where sintering rates vary by a factor of more than 10^6, with an empirically modified version of eq 1.

The modifications required of the German–Munir model must account for additional mechanisms of CaO transport that can proceed concurrently with lattice diffusion and are accelerated by H_2O and CO_2. Whereas the sintering process that occurs in an inert N_2 atmosphere can be described with two parameters, one temperature dependent and the other mechanism dependent, these results show that the latter parameter (γ) also becomes temperature and partial pressure dependent in the presence of H_2O or CO_2.

The relationships between γ and P_{H_2O} or P_{CO_2} indicated by Figure 6 can be combined with those of Figure 9 to give

$$\ln \gamma_{H_2O} = 0.00262T + (\ln P_{H_2O} - 1.39)/11.1 \quad (7)$$

$$\ln \gamma_{CO_2} = 0.0034T + (\ln P_{CO_2} - 1.948)/44.9 \quad (8)$$

which with eq 6 yield γ as a function of temperature and composition of the sintering atmosphere.

Combining eq 3 and 4 gives

$$\ln K_c = 1.485 + 0.558 \ln P_{CO_2} - 11660/T \quad (9)$$

in atmospheres containing both CO_2 and H_2O, subject to the limitation of reaction equilibrium which favors $CaCO_3$ formation at temperatures below 760 °C in 12.2 kPa of CO_2.

Combining eq 7–9 with eq 1, using $S_0 = 76.7$ for hydroxide and 104 for limestone, gives an empirical model for S as a function of time over the range of temperatures required for furnace injection of SO_2 sorbents. This model and measured values for isothermal systems are compared in Table II. The comparisons show a mean difference of 6.3% between predicted surface areas and the measured values (which include experimental error).

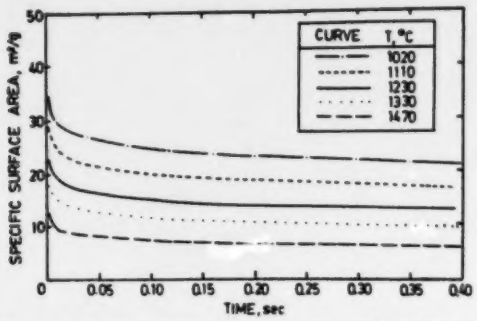

Figure 11. Surface area–time response predicted by sinter model for $Ca(OH)_2$ particles injected into isothermal atmosphere containing 7.3 kPa of H_2O + 12.2 kPa of CO_2. S_0 = 76.7 m^2/g.

All sintering measurements were made at temperatures and partial pressures that preclude the stable formation of $CaCO_3$ or $Ca(OH)_2$, and analyses of the sintered CaO verified their absence. A surface interaction between CaO and H_2O or CO_2 is nevertheless necessary to explain the observed effects. Calculations by Anderson and Morgan (1964) showed that a dynamic adsorption–desorption equilibrium with H_2O is possible in which short-lived surface hydroxyl groups may form. They propose that these groups accelerate the bonding of adjacent CaO lattices to eliminate surface and promote the mobility of O^{2-} along the surface.

The increased sintering rate caused by H_2O or CO_2, especially at lower temperatures, is in qualitative accord with the expected effect of surface diffusion or grain boundary diffusion (Gjostein, 1973; Johnson, 1984; Balluffi, 1984). Relative to the sintering rate of lattice diffusion, these effects are (1) reduction of the apparent activation energy and (2) increase of diffusivity by several orders of magnitude. Thus, a shift of the primary sintering mechanism from slow lattice diffusion to the faster mechanism(s) would agree with the effects apparent from a comparison of Figure 5 with prior data on CaO sintering in N_2, which shows higher slope and lower K_c values at given temperatures. The change in the shape of the S versus t response, reflected by increased γ values at constant temperature, also suggests the influence of surface or grain boundary diffusion.

As previously noted, loss of surface area is more strongly affected by H_2O and CO_2 than is porosity. The data of Table II and Figure 10 nevertheless show that the presence of either gas increases the rate of particle shrinkage relative to that occurring in pure nitrogen. Although surface diffusion might result in a slight shrinkage of grain clusters, it is not expected to cause the large reductions of particle porosity observed, especially those occurring when both H_2O and CO_2 are present. Grain boundary diffusion would be consistent with the observed shrinkage but lacks a plausible means of contact between the boundary surface and atmosphere. The diffusion mechanism induced by the gas interactions cannot therefore be positively identified.

Figure 11 shows the combined effects of H_2O and CO_2 on isothermal sintering of CaO at conditions relevant to furnace injection. The surface areas were calculated with the empirical sinter model (eq 1 and 7–9) for an atmosphere corresponding to the composition of flue gas from coal combustion. The model indicates that most surface reduction occurs in a very short period; at 1230 °C, for example, the initial surface area of 76.7 m^2/g is reduced to 19 m^2/g in about 20 ms.

Application to Nonisothermal CaO Sulfation. Consider the problem in which $Ca(OH)_2$ is injected into a large coal-fired furnace for the purpose of reacting with SO_2 during the passage of CaO and flue gas through the boiler. At normal boiler load, the gas cools at 165 °C/s. To maximize SO_2 capture and sorbent conversion, the $Ca(OH)_2$ must be injected at the highest temperature at which loss of surface area due to sintering does not cancel the effects of longer gas–solid contact and high reaction rate for that surface area. If the coal contains 3.4% sulfur, the initial SO_2 partial pressure is 250 Pa, which limits the maximum temperature of SO_2 capture to 1230 °C—the decomposition temperature of the $CaSO_4$ product. The residence time for SO_2–CaO reaction is therefore less than 2 s before the entrained particles cool to a level where reaction effectively ceases. Given the individual design and operating constraints of the boiler, what is the optimum injection temperature?

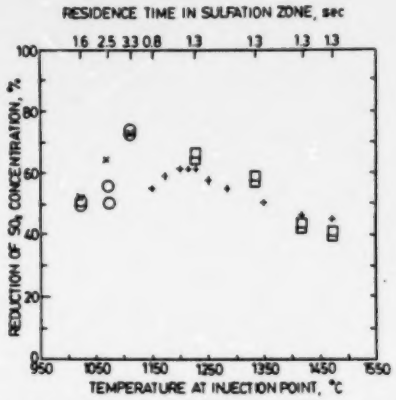
RESIDENCE TIME IN SULFATION ZONE, sec
1.6 2.5 3.3 0.8 1.3 1.3 1.3 1.3
REDUCTION OF SO₂ CONCENTRATION, %
TEMPERATURE AT INJECTION POINT, °C

Figure 12. Comparisons of SO_2 capture predicted by sintering/sulfation models (×, +) with measurements by Beittel et al. (1985) for $Ca(OH)_2$ injection in a coal-fired furnace at 2.2 mol of CaO/SO_2: dT/dt = −52 °C/s (○) and −165 °C/s (□). Particle and gas temperatures assumed equal.

At conversion levels of practical interest, the CaO sulfation rate has been shown to be limited by product layer diffusion (Pigford and Sliger, 1973; Sotirchos and Yu, 1985). When particle size is small enough to eliminate pore diffusion resistance, the conversion versus time response is

$$1 - 3(1 - X)^{2/3} + 2(1 - X) = k_d t \qquad (10)$$

where (Borgwardt and Bruce, 1986; Borgwardt et al., 1987)

$$k_d = 2.65 S^2 P_{SO_2}^{0.84} \exp(-36600/RT) \qquad (11)$$

The sintering model can be applied by approximation to a nonisothermal furnace system to determine the argument S for eq 11 by differentiating eq 1 and rearranging to

$$S = -\left[\int_0^t \frac{K_c S_0}{\gamma}\left(\frac{S_0 - S}{S_0}\right)^{1-\gamma} dt\right] \qquad (12)$$

which can be integrated numerically. In this form, the sintering model was combined with eq 10 and 11 and a sulfur balance to calculate SO_2 capture in a furnace as a function of time and temperature by integration at 5-ms intervals. The results are compared in Figure 12 with experimental data reported by Beittel et al. (1985) for $Ca(OH)_2$ injection in a coal-fired furnace having a well-defined temperature/time profile. The SO_2 reductions measured at normal boiler load (and large dT/dt) are shown as open squares; the circles show performance at

reduced boiler load, which decreases both the temperature and its rate of change at a given injection point. The agreement between these SO_2 measurements and calculated values (×,+) indicates that the model provides an accurate basis for predicting surface area and sulfation rates over the full range of boiler operating conditions.

Additional calculations for normal load operation of the boiler yield an optimum injection temperature of 1200 °C, at which the SO_2 reduction is 61.0% and CaO conversion is 27.8%. The optimum temperature is very close to the decomposition temperature of $CaSO_4$, and equilibrium effects must be considered. These were accounted for in Figure 12 by modifying eq 11 with

$$P_{SO_2} = P^*_{SO_2} - P_e$$

where $P^*_{SO_2}$ is the ambient partial pressure at time t and P_e is the corresponding equilibrium partial pressure given by Coutant et al. (1971):

$$P_e = 218 P_{O_2}^{1/2} \exp(37.46 - 55440/T)$$

assuming particle temperature equal to the gas temperature and unit activities for CaO and $CaSO_4$.

A linear extrapolation of the data of Figure 10 indicates an induction period of about 0.1 s at 1170 °C. At that time (and injection temperature), porosity is still at its maximum value, but the initial stage of sintering has been completed. Thus, the mean diameter of the macropores (and SO_2 pore diffusion rate) will also have maximum values at that point. From these considerations, optimum injection temperature for normal load operation is estimated to be between 1170 and 1200 °C based on gas temperature at the injection point.

Summary and Conclusions

A prior study of the rate of sintering of nascent CaO in a N_2 atmosphere is extended here to include the effects of H_2O and CO_2. The sintering rate at a given temperature is greatly increased by the presence of either gas in the sintering atmosphere and more so by their combination. Both surface area and porosity of the CaO are affected, but the loss of surface area is much faster.

The model of German–Munir, which correlates the kinetics of CaO surface reduction in inert atmospheres, can be modified to account empirically for the effect of H_2O and CO_2. The nature of the modifications suggests that the additional mechanism(s) of transport that are induced by these gases probably involve surface mobility as proposed by Anderson et al. (1965). The effects of temperature and H_2O partial pressure that they reported for MgO sintering are qualitatively similar to those found here for surface reduction during CaO sintering. The overall effects on porosity and surface area observed during sintering in the presence of H_2O and CO_2 suggests that both grain boundary and surface diffusion mechanisms are operative.

Sintering rates obtained in a differential reactor at low temperatures are combined with measurements of Mai (1987) from a high-temperature dispersed-phase reactor to evaluate the effects of temperature and partial pressure over the ranges 380–1150 °C and 39–15000 Pa, respectively. The resulting isothermal model predicts surface area as a function of time and initial properties of $Ca(OH)_2$ and $CaCO_3$ with a mean error of about 6% of the measured values over the full ranges of these variables. The model is extrapolated to higher temperatures and applied to nonisothermal conditions to obtain accurate prediction of SO_2 capture by $Ca(OH)_2$ in a coal-fired furnace by combining with a sulfation rate model that accounts for surface area effects.

The porosity of hydroxide-derived CaO decreased logarithmically with time according to the Coble (1961) model when sintered in a flue gas atmosphere—as was previously shown to be the case for $CaCO_3$-derived CaO sintered in N_2. This reduction of porosity is accelerated by both H_2O and CO_2 and, like surface reduction, is most strongly affected by the combination of both gases. The induction period for porosity loss is expected to be greater than 0.1 s at temperatures up to 1170 °C.

Acknowledgment

I am grateful to Kevin Bruce and Laura Beach of Acurex Corporation for measurement of BET surface area and porosity. Helpful suggestions regarding furnace injection modeling were obtained from Professor Gary Rochelle of the University of Texas at Austin.

Nomenclature

K_c = pseudorate constant for catalyzed sintering in atmospheres containing H_2O and/or CO_2, min^{-1}
k_d = product layer diffusion constant defined by eq 10 and 11
K_i = sintering rate constant for inert atmosphere, min^{-1}
k_p = particle shrinkage constant defined by eq 2
P_e = equilibrium partial pressure of SO_2 over $CaSO_4$, Pa
P_{CO_2} = partial pressure of CO_2 in sintering atmosphere, Pa
P_{H_2O} = partial pressure of H_2O in sintering atmosphere, Pa
P_{O_2} = partial pressure of O_2 in flue gas, kPa
P_{SO_2} = partial pressure of SO_2 above equilibrium partial pressure in flue gas, Pa
$P^*_{SO_2}$ = ambient partial pressure in flue gas at time t, Pa
S = specific surface area at time t, m^2/g
S_0 = initial specific surface area following decomposition of CaO precursor, m^2/g
t = time, min
t_i = induction period for onset of particle shrinkage, min
T = temperature, K
X = CaO conversion to $CaSO_4$, mol fraction

Greek Symbols

γ, γ_{CO_2}, γ_{H_2O}, $\gamma_{CO_2+H_2O}$ = mechanism-dependent exponent of eq 1 correlating surface area and time in atmosphere of N_2, N_2 containing CO_2 or H_2O, and N_2 containing CO_2 and H_2O
ϵ = particle porosity at time t, fraction
ϵ_0 = initial particle porosity following decomposition of CaO precursor

Registry No. H_2O, 7732-18-5; CaO, 1305-78-8; $Ca(OH)_2$, 1305-62-0; CO_2, 124-38-9; SO_2, 7446-09-5.

Literature Cited

Anderson, P. J.; Morgan, P. L. Effects of Water Vapour on Sintering of MgO. *Trans. Faraday Soc.* **1964**, *60*, 930.

Anderson, P. J.; Horlock, R. F.; Avery, R. G. Some Effects of Water Vapour During the Preparation and Calcination of Oxide Powders. *Proc. Br. Ceram. Soc.* **1965**, *3*, 33.

Balluffi, R. W. Grain Boundary Diffusion Mechanisms in Metals. In *Diffusion in Crystalline Solids*; Murch, G. E., Nowick, A. S., Eds.; Academic: New York, 1984.

Beittel, R.; Gooch, J. P.; Dismukes, E. B.; Muzio, L. J. Studies of Sorbent Calcination and SO_2–Sorbent Reactions in a Pilot-Scale Furnace. In *Proceedings: First Joint Symposium on Dry SO_2 and Simultaneous SO_2/NO_x Control Technologies*; US EPA, Air and Energy Engineering Research Laboratory: Research Triangle Park, NC, July 1985; Vol. 1, EPA-600/9-85-020a (NTIS PB 85-232353).

Beruto, D.; Barco, L.; Searcy, A. W. CO_2-Catalyzed Surface Area and Porosity Changes in High-Surface Area CaO Aggregates. *J. Am. Ceram. Soc.* **1984**, *67*, 512.

Borgwardt, R. H. Calcination Kinetics and Surface Area of Dispersed Limestone Particles. *AIChE J.* **1985**, *31*, 103.

Borgwardt, R. H. Sintering of Nascent CaO. *Chem. Eng. Sci.* **1989**, *44*, 53.

Borgwardt, R. H.; Bruce, K. R. Effect of Specific Surface Area on the Reactivity of CaO with SO_3. *AIChE J.* **1986**, *32*, 239.

Borgwardt, R. H.; Bruce, K. R.; Blake, J. An Investigation of Product-Layer Diffusivity for CaO Sulfation. *Ind. Eng. Chem. Res.* **1987**, *26*, 1993.

Borgwardt, R. H.; Roache, N. F.; Bruce, K. R. Method for Variation of Grain Size in Studies of Gas–Solid Reactions Involving CaO. *Ind. Eng. Chem. Fundam.* **1986**, *25*, 165.

Coble, R. L. Sintering in Crystalline Solids, II. Experimental test of diffusion models. *J. Appl. Phys.* **1961**, *32*, 793.

Coutant, R. W.; Simon, R.; Campbell, B.; Barrett, R. E. Investigation of the Reactivity of Limestone and Dolomite for Capturing SO_2 from Flue Gas. EPA Report APTD 0802 (NTIS PB 204385), Oct 1971.

German, R. M.; Munir, Z. A. Surface Area Reduction During Isothermal Sintering. *J. Am. Ceram. Soc.* **1976**, *59*, 379.

Gjostein, N. A. Diffusion. American Society of Metals, Metals Park, OH, 1973.

Johnson, D. L. Ultra Rapid Sintering. In *Sintering in Heterogeneous Catalysis*; Kuczynski, G. C., Miller, A. E., Sargent, G. A., Eds.; Plenum: New York, 1984.

Mai, M. C. Analysis of Simultaneous Calcination, Sintering, and Sulfation of Calcium Hydroxide Under Furnace Sorbent Injection Conditions. Ph.D. Thesis Department of Chemical Engineering, University of Texas at Austin, Austin, TX, 1987.

Nelson, G. O. *Controlled Test Atmospheres*; Ann Arbor Science: Ann Arbor, MI, 1971.

Nicholson, D. Variation of Surface Area During the Thermal Decomposition of Solids. *Trans. Faraday Soc.* **1965**, *61*, 990.

O'Neill, E. P.; Keairns, D. L.; Kittle, W. F. A Thermogravimetric Study of the Sulfation of Limestone and Dolomite—the Effect of Calcination Conditions. *Thermochim. Acta* **1976**, *14*, 209.

Pigford, R. L.; Sliger, G. Rate of Diffusion-Controlled Reaction Between a Gas and a Porous Solid Sphere. *Ind. Eng. Chem. Process Des. Dev.* **1973**, *12*, 85.

Schlaffer, W. G.; Adams, C. R.; Wilson, J. N. Aging of Silica and Alumina Gels. *J. Phys. Chem.* **1965**, *69*, 1530.

Sotirchos, S. V.; Yu, H. C. Mathematical Modelling of Gas–Solid Reactions with Solid Product. *Chem. Eng. Sci.* **1985**, *40*, 2035.

Ulerich, N. H.; O'Neill, E. P.; Keairns, D. L. A Thermogravimetric Study of the Effect of Pore Volume—Pore Size Distribution on the Sulfation of Calcined Limestone. *Thermochim. Acta* **1978**, *26*, 269.

Received for review June 1, 1988
Accepted December 27, 1988